Mon. Not. R. Astron. Soc. **310**, 1147–1152 (1999)

Cold collapse and the core catastrophe

B. Moore,[1] T. Quinn,[2] F. Governato,[3] J. Stadel[2] and G. Lake[2]
[1]*Department of Physics, University of Durham, Durham DH1 3LE*
[2]*Department of Astronomy, University of Washington, Seattle, WA 98195, USA*
[3]*Osservatorio Astronomico di Brera – Merate, Milan, Italy*

Accepted 1999 July 30. Received 1999 June 25; in original form 1999 March 3

ABSTRACT

We show that a universe dominated by cold dark matter fails to reproduce the rotation curves of dark matter dominated galaxies, one of the key problems that it was designed to resolve. We perform numerical simulations of the formation of dark matter haloes, each containing $\gtrsim 10^6$ particles and resolved to 0.003 times the virial radius, allowing an accurate comparison with rotation curve data. A good fit to both Galactic and cluster-sized haloes can be achieved using the density profile $\rho(r) \propto [(r/r_s)^{1.5}(1 + (r/r_s)^{1.5})]^{-1}$, where r_s is a scale radius. This profile has a steeper asymptotic slope, $\rho(r) \propto r^{-1.5}$, and a sharper turn-over than found by lower resolution studies. The central structure of relaxed haloes that form within a hierarchical universe has a remarkably small scatter. We compare the results with a sample of dark matter dominated, low surface brightness (LSB) galaxies with circular velocities in the range 100–300 km s^{-1}. The rotation curves of discs within cold dark matter haloes rise too steeply to match these data, which require a constant mass density in the central regions. The effects of $\Omega_{\rm mass}$ and Λ cannot reconcile the cold dark matter (CDM) model with data – even if we leave the concentration as a free parameter, we are unable to reproduce the observations with such a steep central density profile. It is important to confirm these results using stellar rather than H I rotation curves for LSB galaxies. We test the effects of introducing a cut-off in the power spectrum that may occur in a universe dominated by warm dark matter. In this case, haloes form by a monolithic collapse but the final density profile barely changes, demonstrating that the merger history does not play a role in determining the halo structure.

Key words: galaxies: formation – galaxies: haloes – galaxies: kinematics and dynamics – dark matter.

1 INTRODUCTION

Determining the nature of dark matter remains the most important unsolved problem in modern cosmology. Most baryonic candidates have been ruled out by a variety of dynamical and observational constraints, leaving a host of hypothetical particles as the most popular contenders. Of these, cold dark matter (CDM) remains the primary candidate and provides a highly successful cosmogonic scenario (Davis et al. 1985). The basic premise is an inflationary universe dominated by a dark matter particle, such as the neutralino or axion, that leads to 'bottom up' hierarchical structure formation. Small dense haloes collapse at high redshifts and merge successively into the large virialized systems that can allow gas to cool and form stars and galaxies. The cold dark matter model was originally motivated as a means for providing the mass fluctuation spectrum necessary to form galactic haloes and to explain the large-scale clustering properties of galaxies (Peebles 1984).

A great deal of computational work has been devoted to resolving the structure of haloes that form within the cold dark matter model in order to facilitate a comparison with observational data. The first simulations of Quinn, Salmon & Zurek (1986) and Frenk et al. (1988) did not have the resolution necessary to probe the inner regions of dark haloes that could be compared with galactic rotation curves. However, it was encouraging for the CDM model that the haloes gave flat rotation curves beyond the resolution length of ~50 kpc. Higher resolution simulations by Dubinski & Carlberg (1991), Warren et al. (1992) and Crone, Evrard & Richstone (1994) showed evidence for cuspy density profiles that varied as $\rho(r) \propto r^{-1}$ in the central regions.

Navarro, Frenk & White (1996b, hereafter NFW) made a systematic study of CDM halo structure over a range of mass scales. They found, albeit with a large scatter, that the density profiles of haloes has a universal form, uniquely determined by their mass, varying from r^{-1} in the central regions, smoothly rolling over to r^{-3} at the virial radii. (The virial radius, $r_{\rm vir}$, is

defined as the radius of a sphere that has a mean enclosed density of 200 with respect to the critical value.) Many authors have verified the results of NFW using simulations of a similar resolution, i.e. 5000–20 000 particles per halo and force softening $\sim 0.01 r_{\rm vir}$ (e.g. Cole & Lacey 1996; Tormen, Bouchet & White 1996; Brainerd, Goldberg & Villumsen 1998; Thomas et al. 1998; Jing 1999; etc).

Rotation curves probe the central few per cent of the virial radius; therefore it is important to resolve the formation of this region with more than just a few hundred particles. As the resolution is increased, not only are higher central densities achieved, but the slope of the central density profile increases (Moore et al. 1998). This result was also indicated by high-resolution simulations of isolated halo collapses by Carlberg (1994) and Fukushige & Makino (1997). A large sample of well-resolved, galactic mass haloes analysed by Kravtsov et al. (1998) gave central profiles with slopes shallower than found by NFW, a result that is at odds with the conclusions of this paper.

Most of these studies have found a large variance in the halo structural parameters, depending upon the degree of virialization. The current situation is therefore somewhat confusing. If the cosmological scatter between haloes of the same mass is large, then the Tully–Fisher relation must be somewhat fortuitous, especially in dark matter dominated galaxies such as low surface brightness (LSB) galaxies (e.g. Zwaan et al. 1995; Eisenstein & Loeb 1997; Avila-Reese, Firmani & Hernandez 1998). If the central profiles are steeper than the NFW profile, as the highest resolution studies find, then the hierarchical models will have problems reproducing the observed rotation curves of galaxies.

In this paper we carry out a series of simulations of individual CDM haloes extracted from a large cosmological volume and resimulated at higher resolution. These are the first results for a reasonably large sample of galactic mass haloes, each resolved with $\gtrsim 10^6$ particles and integrated to a redshift $z = 0$. Simulation techniques and parameters are summarized in Section 2. We examine the structure of these haloes and make a comparison with the rotation curves of LSB and dwarf spiral galaxies in Section 3, summarizing our results in Section 4.

2 NUMERICAL TECHNIQUES AND SIMULATION PARAMETERS

Initially we perform a simulation of a 100-Mpc cube of a standard CDM universe with $\Omega = 1$, normalized such that $\sigma_8 = 0.7$ and the shape parameter $\Gamma = 0.5$ (a Hubble constant of $50\,{\rm km\,s^{-1}\,Mpc^{-1}}$ is adopted throughout). The initial simulation contains 144^3 particles with a mass of $2 \times 10^{10}\,{\rm M_\odot}$, and we use a force softening of 60 kpc. The particle distribution is evolved using the parallel treecode PKDGRAV, which has accurate periodic boundaries and variable time-step criteria based upon the local acceleration. The code uses a comoving spline softening length such that the force is completely Newtonian at twice our quoted softening lengths.

At a redshift $z = 0$ we select six haloes with circular velocities in the range 130–230 $\rm km\,s^{-1}$ (total mass $\sim 10^{12}\,{\rm M_\odot}$) that are to be resimulated at higher resolution. Over this range of circular velocities, the NFW simulations predict that the halo concentration should vary by $\lesssim$15 per cent. The haloes we chose lie outside of clusters and voids and are typically within filamentary structures; no pre-selection was made on their merger histories. Two of these haloes are in binary system, with kinematics and environment that resemble the Local Group. As the initial haloes contain just a few hundred particles, we do not know if they will be completely virialized by the final epoch.

The particles that lie within a sphere of radius twice their final virial radii are traced back to the initial conditions to identify the regions that are to be simulated at higher resolution. The power spectrum is extrapolated down to smaller scales, matched at the boundaries such that both the power and waves of the new density field are identical in the region of overlap, then this region is populated with a new subset of less massive particles. Zones of heavier particles are placed outside this region, which allows the correct tidal field to be modelled from the entire cosmological volume of the initial box.

The particle mass in the high-resolution regions is $2 \times 10^6\,{\rm M_\odot}$ and the spline force softening is set to 1 kpc. The starting redshift is increased such that the initial fluctuations are less than 1 per cent of the mean density, typically $z = 100$, and we then rerun the simulation to the present epoch. Each halo requires $\sim$50 000 T3E cpu hours to evolve to the present day. The particles on the shortest time-step require of the order of 50 000 individual steps (see Quinn, Stadel & Lake 1998 for further details of the time-stepping criteria); each calculation requires about 10^{15} floating point operations. The final virial radii of the haloes agree with the low-resolution runs to within a few per cent and even the positions of the largest substructure clumps is accurately reproduced.

3 RESULTS

We identify the halo centres using the most bound particle which agrees extremely well with the centre of mass, recursively calculated using smaller spherical regions. Once the haloes have collapsed, i.e. 90 per cent of their mass is in place, the density profiles do not evolve with time, demonstrating that relaxation does not affect our results even in the central regions. Although a great deal of substructure is evident in these simulations, approximately 85 per cent of the mass within the virial radius lies within a smooth background of particles.

All of the systems we study are completely virialized by a redshift $z = 0$. The largest major accretion of a halo with mass $\gtrsim$25 per cent of the final halo mass occurred over a crossing time before the final time. The density profiles immediately after such an accretion do show strong variations and departures from the final state. However, the disc of a spiral galaxy suffering such a large merger would be destroyed, and by the time a new disc could have reformed, the halo would have achieved a new equilibrium. For this reason we believe that it is important to compare reasonably well-relaxed haloes with rotation curve data.

Fig. 1 shows the rotation curves of our six CDM haloes calculated directly from the particle data, $v_{\rm c}(r) = \sqrt{(GM/r)}$. For each halo we rescale the circular velocities and length-scales by the same factor, such that the peak value is a fiducial $200\,{\rm km\,s^{-1}}$. Our 'average' fiducial galaxy has a virial mass of $1.4 \times 10^{12}\,{\rm M_\odot}$, and a virial radius of 288 kpc, at which point the circular velocity has fallen to $144\,{\rm km\,s^{-1}}$. (This scaling is not unphysical, because the virial radius scales as the circular velocity.) Note that the central rotation curves of the simulated haloes are all very similar; however, the scatter in the total mass is larger. Once scaled to the same peak rotational velocity, the values of the circular velocity at the virial radius vary by 15 per cent , i.e. the total masses vary by $\sim$30 per cent.

In order to compare our results with observational data, we compile a sample of rotation curves of a dozen LSB galaxies with

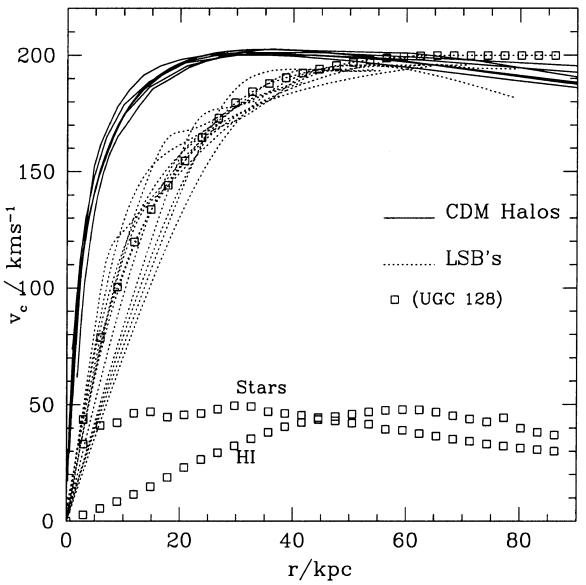

Figure 1. Rotation curves of high-resolution CDM haloes (solid curves) compared with LSB rotation curve data (dotted curves). All of the data and model rotation curves have been scaled to a fiducial peak velocity of $200\,\mathrm{km\,s^{-1}}$. (Note that the simulation haloes and the data were chosen to have peak rotational velocities within 50 per cent of this value.) The total rotational velocity and the baryonic contribution from the stars and gas from a 'typical' LSB galaxy (UGC 128) are shown by the open squares. The mass to baryon ratio for this galaxy is nearly 20:1, and the rotation curve data probes a remarkable 25 per cent of the expected virialized halo.

peak velocities in the range $100–300\,\mathrm{km\,s^{-1}}$. These are taken from de Blok & McGaugh (1997) and Pickering et al. (1997). We treat these rotation curves in the same way as our CDM data, i.e. we rescale lengths and velocities by the same factor to give a peak rotation curve of $200\,\mathrm{km\,s^{-1}}$. In the cases where the peak rotational velocity has not been reached, we adopt a truncated isothermal plus core density profile, and fit the resulting rotation curve to the data in order to estimate the scaling factor. (This would correspond to $\alpha = 2$, $\beta = 3$ and $\gamma = 0$ in equation 1.) We ignore the contribution from the H I gas and stars such that the halo contribution is maximized – including the effects of dissipating baryons only makes the discrepancy between the data and the model worse.

3.1 Dependence on mass, Λ and Ω

Fig. 1 demonstrates that the standard CDM model fails to reproduce the rotation curves of this sample of dark matter dominated galaxies. Lowering the mass density will not solve this problem, because haloes of a given mass would have larger concentrations, as the mean density of the universe is higher during the collapse epoch. Navarro et al. (1996b) find that a flat universe dominated by a cosmological constant leads to haloes with lower concentrations that are marginally consistent with rotation curve data (Navarro 1998). However, the conclusions of Navarro (1998) must be reconsidered in light of the new results in this paper; namely, once haloes are simulated with millions of particles rather than thousands, we find that (i) halo concentrations at a fixed mass are 50 per cent higher and (ii) the central density profiles and therefore circular velocity profiles rise much more steeply.

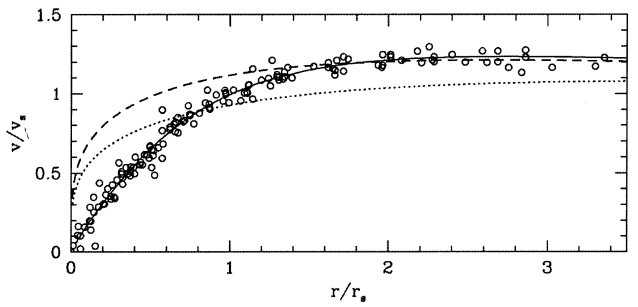

Figure 2. The rotation curves of galaxies, from dwarf spirals to giant LSB galaxies, scaled to fit the universal density profile of equation (1). The solid curve shows the rotation curve that results from a density profile with a constant density core, steepening to a slope of -3 at large radii. The dashed and dotted curves show the rotation curves that result from the density profiles of high-resolution CDM haloes normalized in two different ways. No matter how we rescale the profile, leaving the concentration as a free parameter, we cannot fit these data.

Simulations with $\sim 10^4$ particles per halo indicate that the concentration of CDM haloes is about 30 per cent lower in a Λ-dominated universe (e.g. Jing 1999). We can immediately see that this difference is insufficient to reconcile the data with a hierarchical universe. Including Λ would move the simulated rotation curves less than half-way towards the data points. The beneficial effect of a Λ-dominated universe is more than countered by the higher concentrations found in this paper. Secondly, the discrepancy between data and simulations is exacerbated by the steeply rising density/rotation curves found here. As the form of the density profile (and therefore the rotation curve) is independent of cosmological parameters, we can examine whether there is any value of the concentration that can fit these data. To address this question, we follow Kravtsov et al. (1998) and perform a model-independent rotation curve shape comparison between simulations and data.

The shape of rotation curves of dark matter dominated galaxies is universal across a wide range of galaxy luminosities (Burkert 1995; Persic & Salucci 1997; Kravtsov et al. 1998). Kravtsov et al. (1998) fit a sample of dark matter dominated galaxies to the density profile

$$\rho(r) = \frac{\rho_o}{(r/r_s)^{\gamma}[1 + (r/r_s)^{\alpha}]^{(\beta-\gamma)/\alpha}}, \qquad (1)$$

in order to obtain characteristic scalelengths r_s and circular velocities v_s at r_s. We reproduce their data for dwarf and LSB galaxies in Fig. 2. Although the slope of the density profile in the outer regions is not constrained by these data, a good fit can be obtained using a constant-density central region, i.e. $\alpha = 2$, $\beta = 3$ and $\gamma = 0$. This is indicated by the solid curve that passes through the data points.

We find that the density profiles of our high-resolution haloes are well fitted by a density model in which $\alpha = \gamma = 1.5$ and $\beta = 3$, i.e.

$$\rho(r) = \frac{\rho_o}{[(r/r_s)^{1.5}(1 + (r/r_s)^{1.5})]}. \qquad (2)$$

This profile is plotted in Fig. 2, normalized to produce the same asymptotic flat slope as the data points (dashed curve). We plot the same profile (dotted curve) decreasing the concentration by 60 per cent, twice the expected change from a Λ model. Clearly, whatever way we rescale this profile we cannot reproduce the

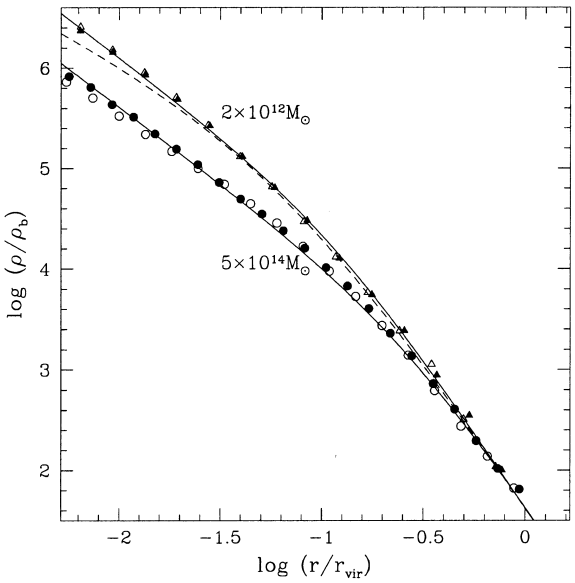

Figure 3. Density profiles of CDM haloes on different mass scales. Open and closed triangles are two similar mass galactic haloes, whilst the filled circles show a cluster mass halo. The open circles show the same cluster halo, but simulated with no power below scales of 8 Mpc. The solid curves show fits to the data using equation (1) with $c_{\rm m} = 10$ for the galaxies and $c_{\rm m} = 4$ for the cluster. The dashed curve indicates an NFW profile fit to the galaxy data for points beyond 3 per cent of the virial radius, in this case $c_{\rm nfw} = 15$.

slowly rising rotation curve data. The only caution that we can offer is that these data are all measured using H I. It would be very difficult to measure these rotation curves using stellar spectroscopy, however, it is very important to verify that the stars are tracing the same potential as the H I.

Fig. 3 shows the density profiles of our two highest resolution galaxy haloes with circular velocities $\sim$220 km s^{-1}, compared with a CDM cluster that has a comparable resolution (Moore et al. 1998). The density profiles of our haloes can be fitted to within a few per cent of the data using equation (2), such that the central profile has a slope -1.5, curving to a slope of -3 at the virial radius. Here, $r_s = r_{\rm vir}/c_{\rm m}$, where for our fiducial galaxy halo we find that a concentration $c_{\rm m} = 10$ fits at all resolved radii (i.e. beyond several softening lengths). The cluster mass halo plotted in Fig. 2 has a virial mass $m_{\rm vir} = 4.3 \times 10^{14}\,{\rm M}_\odot$ within a virial radius $r_{\rm vir} = 1950$ kpc. The peak circular velocity of the cluster is $v_{\rm peak} = 1100$ km s^{-1}, which falls to $v_{\rm vir} = 970$ km s^{-1} at the virial radius. Using equation (2) we find that a concentration $c_{\rm m} = 4.0$ provides a good fit to the density profile.

The NFW density profile ($\alpha = \gamma = 1$ and $\beta = 3$) has a central slope of -1, curving more gently to the asymptotic slope of -3 at the virial radius. If we redefine the concentration such that, in equation (1), $r_s = r_{\rm vir}/c_{\rm nfw}$, we find that for our fiducial galaxy halo a concentration $c_{\rm nfw} = 18$ fits our N-body data to within 20 per cent. This value of the concentration is 50 per cent higher than the 'mean' value predicted by the procedure outlined in Navarro et al. (1996b).

The residuals from the data have a characteristic 'S' shape; underestimating $\rho(r)$ at the halo centre and overestimating $\rho(r)$ in the mid-range. This value for the concentration in the NFW profile gives a slope of -1.2 at 1 kpc, at which point the profile in equation (1) has a slope of -1.6. The 'average' NFW fit to our fiducial halo of this mass should have a concentration $c = 12$. In all cases we find that the best-fitting NFW profile requires a concentration that is 50 per cent larger than the predicted value. This may seem unnecessarily pedantic, but determining the correct central density profile is essential for comparing with observations that probe the inner few per cent of the halo. This is not just an important issue for comparison with galactic rotation curves. For example, the gamma-ray flux from neutralino–neutralino annihilation in the galactic centre is an order of magnitude higher when we use the profiles from our simulated haloes rather than that predicted by NFW.

3.2 The effects of the merger history on halo density profiles

Navarro et al. found that cluster mass haloes have lower concentrations than galaxies, i.e. at a fixed fraction of their virial radius, galaxies are denser than clusters. We also find such a scaling. For comparison with the galactic haloes, we plot one of the cluster simulations from Moore et al. (1998) in Fig. 3. Navarro et al. suggest that clusters are less concentrated than galaxies because they collapse at late times when the universe is less dense. In their scaling model, they take the redshift of collapse as the time when half the mass of the final halo lies in progenitor clumps more massive than a few per cent of the final halo mass.

The results of NFW have stimulated a great deal of theoretical work attempting to explain both the shape of the dark matter density profiles and the scaling with mass and cosmology. Modifications to the self-similar collapse models (i.e. Hoffman & Shaham 1985) to include more realistic dynamics of the growth process have been attempted (cf. Avila-Reese et al. 1998; Henricksen & Widrow 1999; Lokas 1999; Kull 1999, Subramanian, Cen & Ostriker 1999). Several authors argue that the central density profile is linked to the accretion and merging history of dark matter substructure (Syer & White 1998; Salvador-Sole, Solanes & Manrique 1998; Nusser & Sheth 1999). In order to test the importance of the merger history on halo structure, we perform the following experiment. We simulate the evolution of a CDM halo at high resolution using the standard procedure outlined in Section 2. We then resimulate the same halo, but instead of using the full CDM power spectrum extrapolated to small scales, we truncated the spectrum at a scale about half the size of the turnaround region $\equiv$ 8 Mpc.

Although the amplitude of fluctuations is similar on larger scales, the lack of small-scale power causes the halo to form via a single monolithic collapse rather than through mergers and accretions of smaller haloes. This collapse is identical to that taking place in a warm dark matter universe. In this case, the present day free-streaming velocity is negligible and would not provide an additional phase-space constraint on the final core radius (Tremaine & Gunn 1978).

The distribution of mass at redshifts $z = 5$ and $z = 0$ is compared for these two simulations in Fig. 4, and the final density profiles are both plotted in Fig. 3. The virial radii of the two haloes are the same; however, the lack of small scale power is clearly evident in Fig. 4. Remarkably, the final density profiles are also very similar – the halo that formed with no small-scale power has a slightly shallower central slope, -1.4 rather than -1.5. The details of the merger history do not affect the final density profiles.

The concentration of a halo is most likely related to its collapse time; however, the definition of this epoch must be chosen with some care. If we define the collapse time as the epoch at which

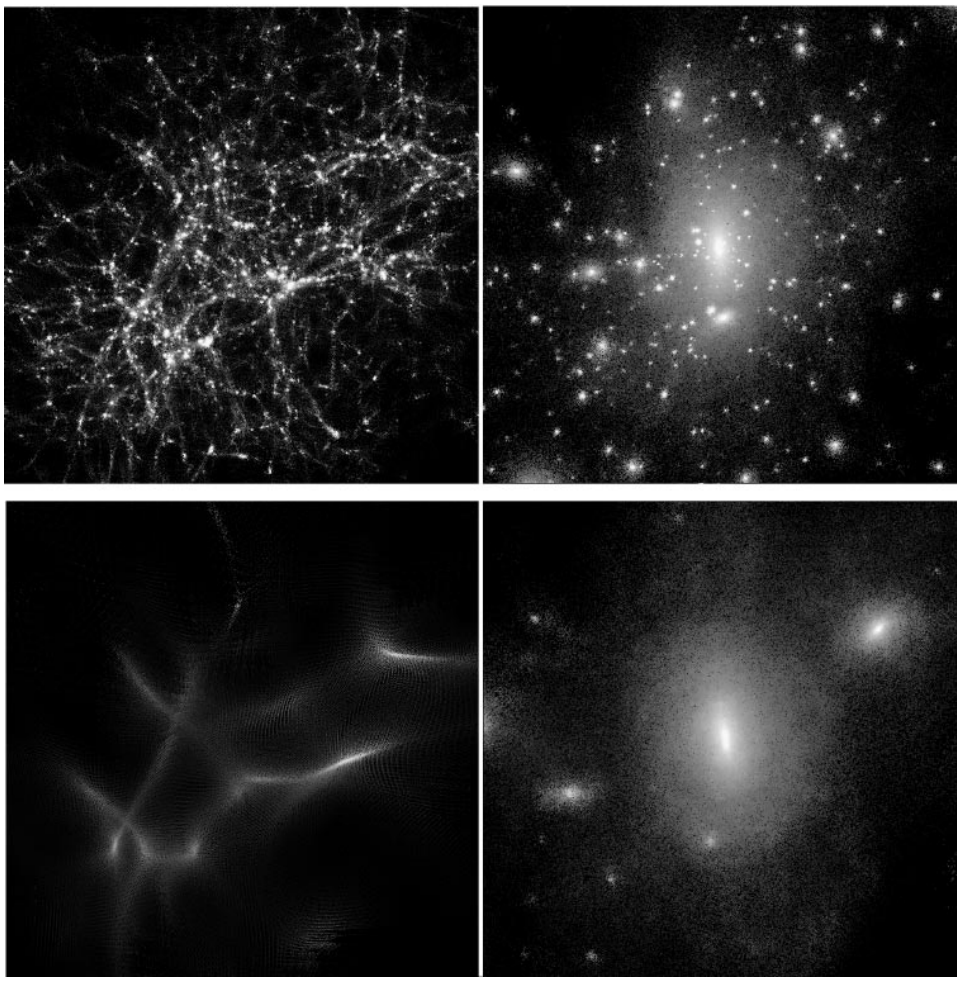

Figure 4. The density field at $z = 5$ (left panels) and $z = 0$ (right panels). The upper plots show the standard CDM halo simulation; the final density profile is plotted as filled circles in Fig. 2. This cluster is the same as analysed by Ghigna et al. (1998). The scale of the left-hand panel is 20 Mpc across, about twice the turnaround region, whereas the right-hand panel is 8 Mpc across and shows the particles within twice the final virial radius. The lower panels show the mass density field at the same epochs and on the same scales, but a cut-off has been placed in the power spectrum. The final density profiles of these haloes are both plotted in Fig. 3.

90 per cent of the mass is in place, then both the haloes simulated in Fig. 4 form at a similar epoch. Defining the collapse time as the epoch when half of the final mass is in smaller collapsed objects is not applicable in this case; at no time is the mass of the second simulation in objects much smaller than the final mass.

Complementary results were also found by Huss, Jain & Steinmetz (1999), who performed a series of tests including isolated halo collapses, hierarchical collapses, varying amounts of substructure and angular momentum. It appears that cuspy central density profiles are a fundamental property of cold gravitational collapse. Neither the amount of small-scale power nor the merger history can create significant changes in the halo density profiles. In order to reproduce the observational data, we must appeal to a new physical process that leads to constant-density cores. Such a mechanism is not inherent in our standard picture of halo formation in cold or warm dark matter cosmologies.

Several authors have investigated the structure of galaxies that form from a cold gravitational collapse of an isolated perturbation (cf. van Albada 1982; Aguilar & Merritt 1990). These simulations typically produced good agreement between the final stellar configuration and the de Vaucouleur $r^{1/4}$ profiles. In three dimensions, this profile has a significantly shallower slope than r^{-1}, and may demonstrate the difference between cold gravitational collapse using cosmological and isolated initial conditions. However, it would be interesting to repeat these tests using the resolution that can be achieved with current resources.

4 SUMMARY AND DISCUSSION

We have performed a series of high-resolution *N*-body simulations of cold dark matter haloes to compare with observations of galactic rotation curves. Our resolution is sufficient to resolve the expected rotation curves over the regions probed by the baryonic component. We find a small scatter in the *central* density profiles, which have asymptotic profiles with a slope $\rho(r) \propto r^{-1.5}$. Recent analysis of a CDM halo simulated with 10^7 particles and a resolution of $0.0005r_{\rm virial}$ demonstrates that this profile has converged (Ghigna et al. 1999).

It is already established that CDM cannot provide the dark matter surrounding dwarf galaxies, because their rotation curves rise more slowly than earlier simulations suggested (Moore 1994; Flores & Primack 1994; Navarro et al. 1996b). Recent proposals to alleviate this problem have included explosive feedback

(Navarro et al. 1996a; Gelato & Sommer-Larson 1999) or reducing the amount of CDM by adding a dark baryonic component (Burkert & Silk 1997).

Low surface brightness galaxies provide the ideal systems for testing the structure of dark matter haloes. They span a range of masses and their luminous components are dominated by dark matter over a large range of radii. The potentials are deep; therefore feedback, however improbable, cannot be invoked as a means of forming central cores. In any case, these galaxies have 'normal' baryon fractions (at least as many baryons as high surface brightness galaxies) and they lie on the Tully–Fisher relationship. Using a compilation of rotation curves provided by Pickering et al. (1997) and de Blok, McGaugh & Van der Hulst (1996), we find that CDM rotation curves rise much too steeply to explain the observational data. Galaxies, such as UGC 128, sample the halo mass distribution to a distance ~25 per cent of the virial radius. Their rotation curves rise slowly within the inner 10–20 kpc, and their rotation curves are best fitted by a large inner region that has a close to constant density.

These galaxies are not rare, and they have properties that connect smoothly into samples of higher surface brightness galaxies. Their surface brightness may result from larger than average angular momentum in the dark matter component. As angular momentum is uncorrelated with both environment and halo structure, we can generalize our results to rule out the possibility that the dark matter in galactic haloes is a cold collisionless particle. Adjusting the cosmological parameters will not change these conclusions, because the shape of the density profile is independent of cosmology and this shape is inconsistent with the observed H I rotation curves. However, these results should be confirmed using stellar velocities of LSB disc stars.

CDM in its current incarnation cannot provide the unknown mass that surrounds galaxies. The dark matter must have an additional property that gives rise to the core–halo structure observed in LSB galaxies. We have shown that cutting the power spectrum such that haloes form from a single monolithic collapse would not change these conclusions; therefore we cannot appeal to warm dark matter models. A phenomenological model that could reproduce the observations would be to invoke a dark matter particle with a large cross-section for annihilation into 'hot dark matter'. The mass annihilation rate varies as $\rho^2\sigma$, where σ is the central velocity dispersion. The annihilation by-products would stream from the halo centres, leaving a core radius that correlated directly with the circular velocity modulo a factor proportional to the collapse time. This would also resolve the problem of the overabundance of dark matter substructure haloes in CDM models, because these would suffer early tidal disruption once within the virial radius (Moore et al. 1999).

ACKNOWLEDGMENTS

We thank all of our colleagues for stimulating discussions on dark matter haloes. We also thank Stacy McGaugh and Tim Pickering for providing rotation curve data and comments and Andrey Kravtsov for providing additional data for Fig. 3. The numerical simulations required many cpu hours, which were primarily obtained as part of the Virgo consortium. BM is a Royal Society Research Fellow.

REFERENCES

Aguilar L. A., Merritt D., 1990, ApJ, 354, 33
Avila-Reese V., Firmani C., Hernandez X., 1998, ApJ, 505, 37
Brainerd T. G., Goldberg D. M., Villumsen J. V., 1998, ApJ, 502, 505
Burkert A., 1995, ApJ, 447, L25
Burkert A., Silk J., 1997, ApJ, 488, L55
Carlberg R., 1994, ApJ, 433, 468
Cole S., Lacey C., 1996, MNRAS, 281, 716
Crone M. M., Evrard A. E., Richstone D. O., 1994, ApJ, 434, 402
Davis M., Efstathiou G., Frenk C. S., White S. D. M., 1985, ApJ, 292, 371
de Blok W. J. G., McGaugh S. S., 1997, MNRAS, 290, 533
de Blok W. J. G., McGaugh S. S., Van der Hulst J. M., 1996, MNRAS, 283, 18
Dubinski J., Carlberg R., 1991, ApJ, 378, 496
Eisenstein D. J., Loeb A., 1997, ApJ, 459, 432
Evans W. N., Collet J. L., 1997, ApJ, 480, L103
Flores R. A., Primack J. R., 1994, ApJ, 457, L5
Frenk C. S., White S. D. M., Davis M., Efstathiou G., 1988, ApJ, 327, 507
Fukushige T., Makino J., 1997, ApJ, 477, L9
Gelato S., Sommer-Larson J., 1999, MNRAS, 303, 321
Ghigna S., Moore B., Governato F., Lake G., Quinn T., Stadel J., 1998, MNRAS, 300, 146
Ghigna S., Moore B., Governato F., Quinn T., Stadel J., Lake G., 1999, ApJ, submitted
Henriksen R. N., Widrow L. M., 1999, MNRAS, 302, 321
Hoffman Y., Shaham J., 1985, ApJ, 297, 16
Huss A., Jain B., Steinmetz M., 1999, ApJ, in press
Jing Y. P., 1999, ApJ, submitted
Kull A., 1999, ApJL, in press
Kravtsov A. V., Klypin A. A., Bullock J. S., Primack J. R., 1998, ApJ, 502, 48
Lokas E. L., 1999, MNRAS, submitted
Moore B., 1994, Nat, 370, 620
Moore B., Governato F., Quinn T., Stadel J., Lake G., 1998, ApJ, 499, L5
Moore B., Ghigna S., Governato F., Lake G., Quinn T., Stadel J., Tozzi P., 1999, ApJ, 524, L19
Navarro J. F., 1998, ApJ, submitted
Navarro J. F., Eke V. R., Frenk C. S., 1996a, MNRAS, 283, L72
Navarro J. F., Frenk C. S., White S. D. M., 1996b, ApJ, 462, 563
Nusser A., Sheth R., 1999, MNRAS, 303, 685
Peebles P. J. E., 1984, ApJ, 277, 470
Persic M., Salucci P., 1997, in Persic M., Salucci P., eds, ASP Conf. Ser. Vol. 117, Dark and Visible Matter in Galaxies. Astron. Soc. Pac., San Francisco, p. 1
Pickering T. E., Impey C. D., Van Gorkom J. H., Bothun G. D., 1997, AJ, 114
Quinn P. J., Salmon J. K., Zurek W. H., 1986, Nat, 322, 329
Quinn T., Stadel J., Lake G., 1998, ApJ, submitted
Salvador-Sole E., Solanes J. M., Manrique A., 1998, ApJ, 499, 542
Syer D., White S. D. M., 1998, MNRAS, 293, 337
Thomas P. et al., 1998, MNRAS, 296, 1061
Tormen G., Bouchet F. R., White S. D. M., 1996, MNRAS, 286, 865
Tremaine S., Gunn J. E., 1978, Phys. Rev. Lett., 42, 407
Van Albada T. S., 1982, MNRAS, 201, 939
Warren S. W., Quinn P. J., Salmon J. K., Zurek H. W., 1992, ApJ, 399, 405
Zwaan M. A., van der Hulst J. M., de Blok W. J. G., McGaugh S. S., 1995, MNRAS, 273, L35

This paper has been typeset from a TEX/LATEX file prepared by the author.